Random flights in confining interfacial systems

2005 J. Phys.: Condens. Matter 17 S4059

(http://iopscience.iop.org/0953-8984/17/49/004)

INSTITUTE OF PHYSICS PUBLISHING JOURNAL OF PHYSICS: CONDENSED MATTER

J. Phys.: Condens. Matter **17** (2005) S4059–S4074 doi:10.1088/0953-8984/17/49/004

Random flights in confining interfacial systems

Pierre Levitz

Laboratoire de Physique de la Matière Condensée, UMR 7643 du CNRS-Ecole Polytechnique, 91128 Palaiseau, France

E-mail: levitz@pmc.polytechnique.fr

Received 11 July 2005
Published 25 November 2005
Online at stacks.iop.org/JPhysCM/17/S4059

Abstract

Porous materials, concentrated colloidal suspensions are examples of confining systems developing large specific surface and presenting a rich variety of shapes. Such an interfacial confinement strongly influences the molecular dynamics of embedded fluids and the diffusive motion of entrapped Brownian particles. An individual trajectory near the interface can be described as an alternate succession of adsorption steps and random flights in the bulk. Statistical properties of these random flights in various interfacial confining systems are needed as prerequisites in order to understand the full transport process. Related to first passage processes, these properties play a central role in numerous problems such as the mean first exit time in a bounded domain, heterogeneous catalytic reactivity and nuclear magnetic relaxation in complex and biological fluids. In the present work, we first consider the various possibilities of connecting two points of a smooth interface by a random flight in the bulk. Second, we analyse from the theoretical and experimental points of view a way to probe Brownian flight statistics. From the experimental point of view, we investigate the slow fluid dynamics near some colloidal interfaces by field-cycling NMR relaxometry. This is a way to follow slow dynamical correlations from 1 ns to 10 μs. This spectroscopy appears to be a good choice, considering that the algebraic nature of the probability of the first return to a surface builds a long-time memory. The experimental part confirms that the embedded fluid dynamics is sensitive to possible morphologic crossover and provides information about interface geometry. We also believe that such an approach can be used to probe interfacial dynamics by itself, for example in the case of a colloidal system undergoing a phase transition (dynamical arrest, rotational blockage, . . .).

1. Introduction

Porous materials and colloidal suspensions are examples of confining systems developing large specific surface, presenting a rich variety of shapes and exhibiting complex and irregular

morphologies on a large length scale. Such a confinement strongly influences the molecular dynamics of embedded fluids and the diffusive motion of Brownian particles entrapped inside these materials. Diffusion transport plays a crucial role in various transport phenomena in nature and industry [1, 2].

In this general frame, a close inspection of particle and or molecular trajectories is instructive. The particle reaches the interface after a random walk in the bulk. It can be either adsorbed or transferred with some probability or it can be reflected, performing a new diffusion step in the bulk. Until definitive loss by adsorption or final escaping, the particle trajectory can be described as an alternate succession of surface encounters and flights in the bulk (also called loops in this paper). The statistics of times and the displacements between two interface hits are needed as prerequisites in order to understand the full transport process. This question is related to a first passage problem [3] and plays a central role in thermodynamics of rough colloidal surfaces [4, 5], in the evaluation of the mean first exit time from a bounded domain [8, 6, 7] or in better understanding of nuclear magnetic relaxation processes in complex fluids and porous media [12, 9]. Interestingly enough, these loop statistics have to be used whatever the surface boundary conditions are, ranging from strong adsorption (Dirichlet) to complete reflection (Neumann) with the intermediate situation of partially reflected motion.

In the present work, we review some statistical properties of these random flights in various interfacial confining systems. First, we consider the various possibilities of connecting two points of a smooth interface by a random flight in the bulk and we recall some recent results concerning Pearson random walk statistics. Second, we analyse from the theoretical and experimental points of view a way to probe Brownian flight statistics. Some experimental results are then presented. Last, we discuss how surface shape and interface irregularities can affect the loop statistics and induce, at long times, specific transport properties.

2. Random flights and first passage statistics

There are numerous ways to connect two points of an interface by a random flight in the bulk. Gas diffusion in confining geometry provides a good illustration of these various transport regimes. At very low pressure, in the Knudsen regime, a gas molecule connects two distinct points of the interface by a straight line, called a chord. Diffuse reflection conditions at the interface and the chord length distribution function [11–13] determine the randomness of the molecular trajectory. In contrast, at high pressure, the mean free path λ of a molecule is well below the mean pore chord length $\langle l_p \rangle$. The so-called Knudsen number $Knu = \lambda/\langle l_p \rangle$ goes to zero and the molecule is mainly submitted at stochastic distances to random reorientation and reinitialization of its velocity according to a stable Maxwell–Bolztmann distribution. The stochastic distances are exponentially distributed with a mean value λ. This regime is very close to a Brownian flight between two points of the interface.

We have simulated the diffusion of a gas molecule inside a sphere of diameter $2R$. A large domain of variation of the Knudsen number was explored. We have computed the probability distribution functions (pdfs) characterizing the time ($\psi_L(t)$) and distance ($\theta_L(r)$) distribution between two interface hits. In the Knudsen regime (see figures 1 and 2), we find a linear dependence of these two pdfs which is imposed by the linear evolution of the chord length distribution between the origin and $2R$. For Knu close to zero, i.e. in the molecular regime, the probability distribution $\psi_L(t)$ evolves as $1/t^{1.5}$ over a large range of time. Meanwhile, the probability distribution of displacements $\theta_L(r)$ runs as $1/r^2$ where r is the end to end distance of a bulk loop. This last function exhibits a cut-off for a distance close to the diameter of this bounded domain. For this smooth and curved surface, we find a well-known result predicted a long time ago in the case of a infinite flat surface [14] (Cauchy distributions) and recently

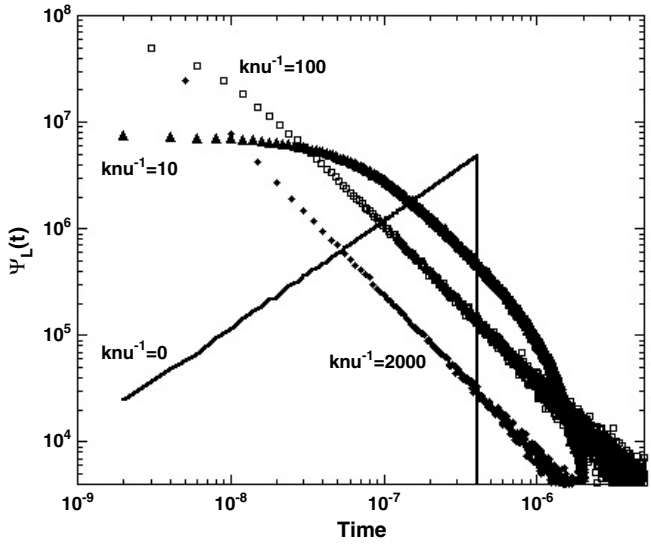

Figure 1. Evolution of the probability distribution $\psi_{\mathrm{L}}(t)$ that a particle starts from the interface at $t = 0$ and returns to it, for the first time, at time between t and $t + \mathrm{d}t$. Comparison between different gas diffusion regimes inside a sphere of diameter $2R$. The Knudsen regime is observable for $Knu^{-1} = 0$ and a Brownian random walk is reached for $Knu^{-1} = 2000$.

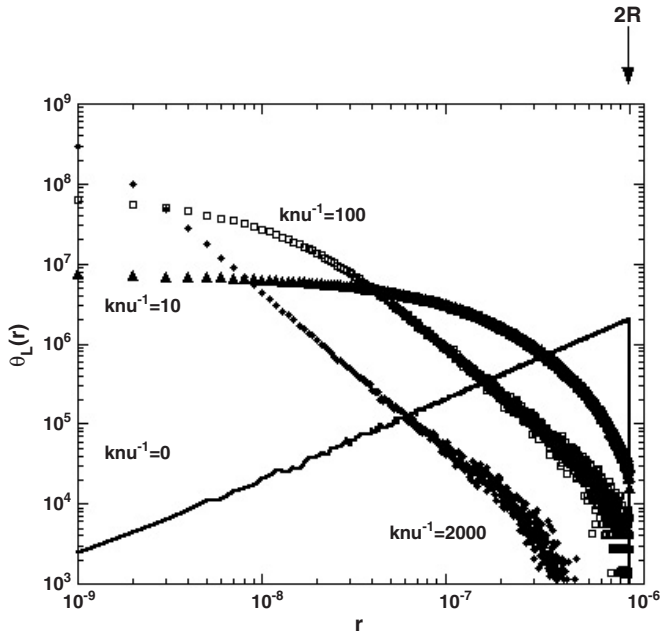

Figure 2. Evolution of the probability distribution $\theta_{\mathrm{L}}(r)$ where r is the end to end Euclidean distance of a bulk. Comparison between different gas diffusion regimes inside a sphere of diameter $2R$. The Knudsen regime is observable for $Knu^{-1} = 0$ and an Brownian random walk is reached for $Knu^{-1} = 2000$.

discussed in detail by Bychuk and O'Shaughnessy [15, 16]. The finite persistence length of the interface and the finite size of this bounded domain introduce a natural upper cut-off avoiding

the divergence of the first (the average time of a flight) and second moment of $\psi_L(t)$. For a bounded domain of diffusion, the first moment of $\psi_L(t)$ is also the mean first exit time of a random walk starting from the interface. We can check using data shown in figure 1 that this first moment is almost independent of the mean free path λ and is directly connected to the specific surface of this interfacial system. This result was recently demonstrated in the literature in the case of Pearson random walks [6–8].

In the Knudsen regime, $\psi_L(t)$ and $\theta_L(r)$ are simply connected using the basic relation $r = \langle v \rangle t$, where $\langle v \rangle$ is the mean molecular velocity of the gas [13]. In the opposite regime, the Fourier transform $\tilde{\theta}_L(k)$ of $\theta_L(r)$ can be related to $\psi_L(t)$ through the diffusion Green's function [16]:

$$\tilde{\theta}_L(k) = \int_0^\infty \mathrm{d}t\ \psi_L(t)\ \exp(-Dk^2 t). \tag{1}$$

This equality assumes that the Brownian dynamics in the bulk is not biased by the confinement of the interface. To be more general, let us consider that $\psi_L(t) \sim t^{-\alpha}$ and $\theta_L(r) \sim r^{-\beta}$ for large enough t and r. Using equation (1), it is easy to see that these two exponents are simply connected. If we substitute $s = Dk^2$ in equation (1), then the use of the ansatz $\psi_L(t) = t^{-\alpha}$ and the Tauberian estimates [14] leads to $\tilde{\theta}_L(s) \sim 1 - s^{\alpha-1}$. Taking the inverse Fourier transform we get:

$$\theta_L(r) = \int_{-\infty}^\infty \mathrm{d}k\, \tilde{\theta}_L(k) \exp(-\mathrm{i}kr) \sim \frac{1}{r^{1+2(\alpha-1)}}. \tag{2}$$

This gives us

$$\beta = 2\alpha - 1. \tag{3}$$

The validity of this scaling equality was recently checked in the case of irregular and fractal interfaces [25].

3. A way to probe Brownian flights

3.1. Possible strategy

We will now consider the case of Brownian random walks in confinement where the trajectory near an interface can be described as an alternate succession of adsorption steps and Brownian flights in the bulk. As shown elsewhere [9, 17], the nuclear magnetic relaxation dispersion (NMRD) technique is an effective experimental method for following such a bulk mediated surface diffusion.

During its self-diffusion, a nuclear spin-bearing fluid molecule experiences a local fluctuating magnetic interaction $I(t)$. In the simplest case, $I(t)$ is a scalar interaction which takes a defined value during the adsorption step (A) and vanishes during the bulk loop (L). This situation is shown in part (A) of figure 3. $I(t)$ appears as an alternate sum of Heaviside distributions $H(t)$ with the same amplitude. $I(t)$ can be also a tensorial interaction involving for example a quadrupolar or an intra-dipolar magnetic interaction. In these two cases, it is possible to show that $I(t)$ is meanly sensitive (in the slow dynamic limit) to the time evolution of the surface director probed by the molecule during its self-diffusion. As shown in the right part of figure 3, $I(t)$ takes a specific value for each encounter with the surface directly related to the local surface orientation. Curvature, persistence length and roughness of a surface can then be probed by random flights. The basic case of a flat surface is interesting. For an immobile surface, $I(t)$ evolves according to the scheme of figure 3(A). Rotation of the interface will induce a specific modulation of the magnetic noise $I(t)$ directly related to the surface dynamics.

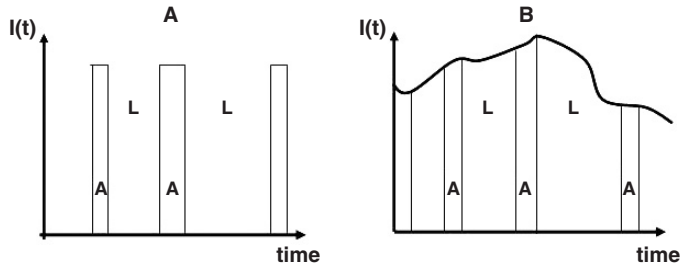

Figure 3. Slow component of a magnetic fluctuation probed by a fluid molecule near a flat interface. A and L stand for the adsorption stage and for the Brownian loop in the bulk, respectively. In (A), $I(t)$ is a scalar interaction which takes a defined value during the adsorption step. In (B), $I(t)$ is either an intra-dipolar or a quadrupolar interaction and takes a specific value for each encounter with the surface.

The magnetic fluctuation will then evolve according to figure 3(B). A sensitive way to probe the temporal fluctuation of $I(t)$ is to look at the spectral density of this magnetic noise. This noise induces a nuclear magnetic relaxation process at the Larmor frequency ω (with $\omega = 2\pi f$). Using field-cycling NMR spectroscopy [9, 17], the related spin-lattice relaxation rate $R_1(\omega)$ can be measured over a large range of frequencies ω, mainly from a few kHz to several hundred MHz. This frequency range allows us to probe correlation times ranging from 1 ns to tenths μs. Following [18], the spin-lattice relaxation rate can be decomposed, at low frequency, into a fast and a slow contribution statistically independent, such as $R_1(\omega) = R_1^{\text{slow}}(\omega) + R_1^{\text{fast}}$. The fast contribution is related to local molecular dynamics and is almost constant at low frequency. The slow motion contribution can be written as $R_1^{\text{slow}}(\omega) \propto J(\omega) + 4J(2\omega)$, where $J(\omega)$ is the time Fourier transform of the correlation function $\langle I(t) * I(-t)\rangle$, where $*$ stands for the convolution operator. This last equality offers an experimental way to probe the statistical properties of $I(t)$. In the two following sections, we will see how $J(\omega)$ or $R_1^{\text{slow}}(\omega)$ are sensitive to random flight statistics and depend on $\psi_{\text{L}}(t)$.

3.2. Case of an unbounded interface

In this section, we analyse the case of a fluid molecule interacting with an unbounded interface through a scalar interaction. This situation is shown in figure 3(A). The 'relaxation noise', $I(t)$, thus appears as an alternate sum of Heaviside distributions $H(t)$ with the same amplitude. A typical occurrence of $I(t)$ can be written as $I(t) = L(t)$ with $L(t) = \sum_i (-1)^i H(t - t_i)$. The particle encounters the surface for an adsorption step during typical time intervals $]t_{2i}, t_{2i+1}[$ or leaves it for a bulk loop according to typical time intervals $]t_{2i+1}, t_{2i+2}[$.

In order to get $J(\omega)$, we first compute the second derivative of the self-correlation function $\langle I(t) * I(-t)\rangle$ according to [11]:

$$\langle I(t) * I(-t)\rangle'' = L_2''(t) = -\langle I'(t) * I'(-t)\rangle = \sum_{i,j} (-1)^{i+j} \delta(t - (t_i - t_j)). \tag{4}$$

Assuming no correlation between successive temporal events (i.e. adsorption steps followed by a bulk excursion), we compute the following ensemble averages:

$$\begin{aligned}
&\langle \delta(t - (t_{2j+1} - t_{2j}))\rangle = \psi_{\text{A}}(t) \\
&\langle \delta(t - (t_{2j+2} - t_{2j+1}))\rangle = \psi_{\text{L}}(t) \\
&\langle \delta(t - (t_{2j+2} - t_{2j}))\rangle = \psi_{\text{A}}(t) * \psi_{\text{L}}(t) \\
&\langle \delta(t - (t_{2j+3} - t_{2j+1}))\rangle = \psi_{\text{L}}(t) * \psi_{\text{A}}(t) \ldots
\end{aligned} \tag{5}$$

where $\psi_A(t)$ is the pdf characterizing the adsorption time distribution. The second time derivative $L_2''(t)$ is a even function and can written for $t \geqslant 0$ as:

$$L_2''(t) \propto -2\delta(t) + \psi_A(t) + \psi_L(t) - 2\psi_A(t) * \psi_L(t) + \psi_L(t) * \psi_A(t) * \psi_L(t) + \psi_A(t) * \psi_L(t) * \psi_A(t) - \cdots \quad (6)$$

and for $t \leqslant 0$ as:

$$L_2''(t) \propto -2\delta(t) + \psi_A(-t) + \psi_L(-t) - 2\psi_A(-t) * \psi_L(-t) + \psi_L(-t) * \psi_A(-t) * \psi_L(-t) + \psi_A(-t) * \psi_L(-t) * \psi_A(-t) - \cdots. \quad (7)$$

The time Fourier transform of $L_2''(t)$ denoted $\tilde{L}_2''(\omega)$ is given by:

$$\tilde{L}_2''(\omega) \propto -2 + 2\,\mathrm{Re}(\tilde{\psi}_A(\omega) + \tilde{\psi}_L(\omega) - 2\tilde{\psi}_A(\omega)\tilde{\psi}_L(\omega) + \tilde{\psi}_L^2(\omega)\tilde{\psi}_A(\omega) + \tilde{\psi}_A^2(\omega)\tilde{\psi}_L(\omega) - \cdots \quad (8)$$

where $\tilde{\psi}_L(\omega)$ and $\tilde{\psi}_A(\omega)$ are the time Fourier transforms of the two pdfs characterizing the loop statistics and the adsorption step respectively. Equation (8) can be simplified as:

$$\tilde{L}_2''(\omega) \propto -\mathrm{Re}\left[\frac{(1-\tilde{\Psi}_L(\omega))(1-\tilde{\Psi}_A(\omega))}{1-\tilde{\Psi}_L(\omega)\tilde{\Psi}_A(\omega)}\right]. \quad (9)$$

We get:

$$\tilde{L}_2(\omega) = \frac{\sigma}{\omega^2}\,\mathrm{Re}\left[\frac{(1-\tilde{\Psi}_L(\omega))(1-\tilde{\Psi}_A(\omega))}{1-\tilde{\Psi}_L(\omega)\tilde{\Psi}_A(\omega)}\right]. \quad (10)$$

σ is a constant taking into account the strength of the magnetic interaction during the adsorption step.

As discussed in section 2, let us consider that we have, at long times, $\psi_L(t) = (\mu\tau_L^{\mu})/t^{(1+\mu)}$, where τ_L is the minimal loop duration. A basic and usual choice is to consider that $\psi_A(t) = (1/\tau_A)\exp(-t/\tau_A)$, where τ_A is the average adsorption time. Asymptotic expansions of $\tilde{\psi}_L(\omega)$ and $\tilde{\Psi}_A(\omega)$ for small ω values and any value of μ between 1 and 2 reads:

$$\tilde{\psi}_L(\omega) = (1 - a(\mu)) + \mathrm{i}b(\mu)\omega^{\mu} \quad (11)$$

with

$$a(\mu) = |\Gamma(-\mu)|\cos(\pi\mu/2)\mu\tau_L^{\mu}, \quad b(\mu) = |\Gamma(-\mu)|\sin(\pi\mu/2)\mu\tau_L^{\mu} \quad (12)$$

and

$$\tilde{\psi}_A(\omega) = (1 - \omega^2\tau_A^2) + \mathrm{i}\omega\tau_A. \quad (13)$$

Γ stands for the Gamma function. After some tedious but straightforward computations we finally get:

$$\tilde{L}_2(\omega) = \frac{\sigma\tau_A^2}{a(\mu)(1 + b(\mu)^2\omega^{\mu}/a(\mu)^2) + (2\tau_A b(\mu)\omega/a(\mu)) + (\tau_A^2\omega^{2-\mu}/a(\mu))}. \quad (14)$$

In the specific case of a flat interface where $\mu = 1/2$, we obtain:

$$J(\omega) = \tilde{L}_2(\omega) = \frac{\sigma\tau_A/2\omega_0}{[(\omega/\omega_0)^{1/2} + (\omega/\omega_0) + 1/2(\omega/\omega_0)^{3/2}]} \quad (15)$$

where ω_0 is a characteristic frequency written as $\omega_0 = \Gamma^2(1/2)\tau_L/2\tau_A^2$. At low frequencies ($\omega \ll \omega_0$), $\tilde{L}_2(\omega)$ evolves as $1/\sqrt{\omega}$. Around ω_0, we have a $1/\omega$ regime. Finally, for $\omega \gg \omega_0$, $\tilde{L}_2(\omega)$ is dominated by the term $1/\omega^{3/2}$.

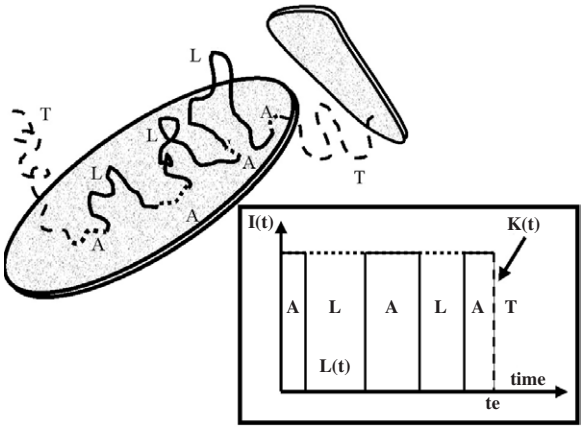

Figure 4. Fluid trajectory at proximity of an finite flat interface. A: adsorption step; L: Brownian loop in the bulk relative to the finite interface; T: escaping tail from the finite interface. In the inset, a statistical occurrence of the noise, $I(t)$, product of an alternate sum of Heaviside functions, $L(t)$, and a cut-off function $K(t)$. t_e is the overall escaping time from the particle, associated to the considered occurrence.

3.3. Finite interface and escaping process

Let us now consider a finite interface as shown in figure 4. Two escaping tails (T) begin and end the overall exploration of this interface. The 'relaxation noise', $I(t)$, is now bounded by a cut-off function $K(t)$ that takes into account the possibility of leaving definitively the finite flat interface. $K(t)$ equals unity between two escaping tails and zero elsewhere. A typical occurrence of $I(t)$ can be written as $I(t) = K(t) \cdot L(t)$. In order to compute $J(\omega)$, the statistical independence of the two random functions $L(t)$ and $K(t)$ is assumed. We use the following approximation:

$$\langle I(t) * I(-t)\rangle = \langle (L(t)\cdot K(t)) * (L(-t)K(-t))\rangle \sim \langle L(t) * (L(-t)\rangle\langle K(t) * K(-t)\rangle. \quad (16)$$

The validity of these relations was checked numerically. Generation of a large number of alternate series of time intervals chosen according to algebraic $\psi_L(t)$ and exponential $\psi_A(t)$ was first performed. $\langle I(t) * I(-t)\rangle$, $L_2(t) = \langle L(t) * L(-t)\rangle$ and $C_{esc} = \langle K(t) * K(-t)\rangle$ were computed. Finally, and as shown in figure 5, equation (16) appears to be a good approximation.

The ensemble average $\langle K(t)\rangle$ is the overall survival probability $S(t)$ near the finite surface. $C_{esc}(t) = \langle K(t) * K(-t)\rangle$ can be written as

$$C_{esc}(t) = -\int_t^\infty S'(t_e)(t_e - t)\,dt_e = \int_t^\infty S(t_e)\,dt_e. \quad (17)$$

Finally,

$$J(\omega) = \tilde{C}_{esc}(\omega) * \tilde{L}_2(\omega) \quad (18)$$

where $\tilde{L}_2(\omega)$ is given by equation (14).

The approximation proposed in equation (16) can be used to analyse the general case shown in figure 3(B). $J(\omega)$ can be generalized as $\tilde{C}_{orien}(\omega) * \tilde{C}_{esc}(\omega) * \tilde{L}_2(\omega)$. $\tilde{C}_{orien}(\omega)$ is the time Fourier transform of $C_{orien}(t)$ which takes into account the variation of the magnetic interaction magnitude in time and/or in space. Such a situation can be encountered in the case of fluctuating interfaces [10] or for disordered, multi-connected or rough confining interfacial systems.

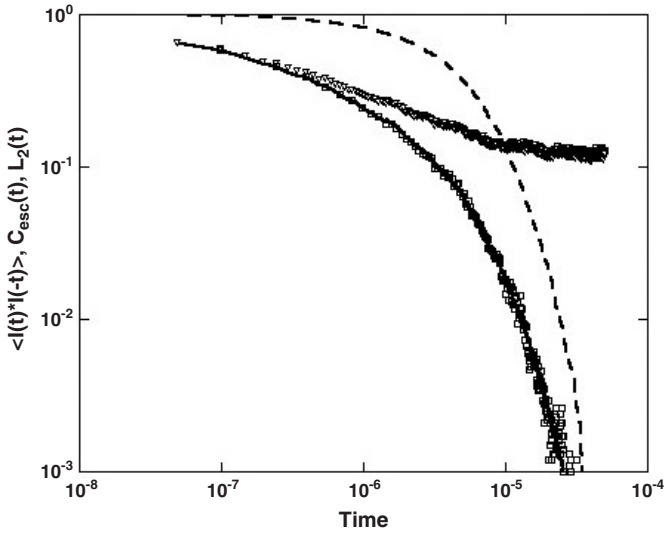

Figure 5. 1D numerical computation of $\langle I(t) * I(-t)\rangle$ (open squares), $L_2(t) = \langle L(t) * (L(-t)\rangle$ (open triangles) and $C_{\rm esc}(t) = \langle K(t) * K(-t)\rangle$ (dotted line) after generation of a large number of alternate series of time intervals chosen according to algebraic $\psi_{\rm L}(t)$ and exponential $\psi_{\rm A}(t)$. The product $L_2(t)C_{\rm esc}(t)$ (continuous line) is very close to $\langle I(t) * I(-t)\rangle$.

4. Some experimental and numerical results

The simplest way to investigate the random flight statistics close to an interface is to look at the dynamics near a macroscopic plane surface. However, such an experimental model is not sufficiently sensitive. We have chosen to work with an aqueous colloidal suspension of flat and thin particles called laponite [19, 20]. This synthetic clay particle can be considered, on average, as a negatively charged platelet, 1 nm thick, with an average diameter around 25–30 nm. For an ionic strength of 10^{-4} M) and above the concentration threshold of 0.01 w/w, one observes a jamming and/or a glass transition associated to a strong slowing down of the particle dynamics. We have measured the proton and deuterium NMRD in several laponite colloidal glasses. Measurements were performed, at 298 K, on a fast field-cycling spectrometer from Stelar Company. Proton (H20) and deuterium (D20) NMRD are similar. This proves that the proton relaxation process is mainly due to the intramolecular proton–proton interaction as required in our theoretical model. Figure 6 shows a typical evolution of the 1H NMRD dispersions in the glass 'phase'. A leveling-off regime appears below a crossover frequency $f_{\rm c} \sim 40$ kHz, Above this threshold, $R_1(\omega)$ evolves mainly as $\omega^{-1} + Cte$. The constant takes into account the spin-lattice relaxation rate associated to rapid molecular dynamics. As shown in the inset of figure 6, the use of the frequency derivative of R_1 is an efficient way to exhibit specific contributions of slow dynamics and especially the algebraic regime.

In parallel to the experimental investigation, a simulated annealing algorithm in reciprocal q-space has been successfully developed allowing us to generate 3D off-lattice configurations of laponite suspensions having neutron small-angle scattering spectra similar to the experimental ones [21, 22]. Moreover, a supplementary constraint, imposing a defined nematic order parameter $S_{\rm ord}$, was added. Three different configurations are shown in figure 7. We have simulated the self-diffusion of an embedded fluid molecule inside these confining interfacial systems. Brownian dynamics, with a time step of 5 ps, is performed to follow the

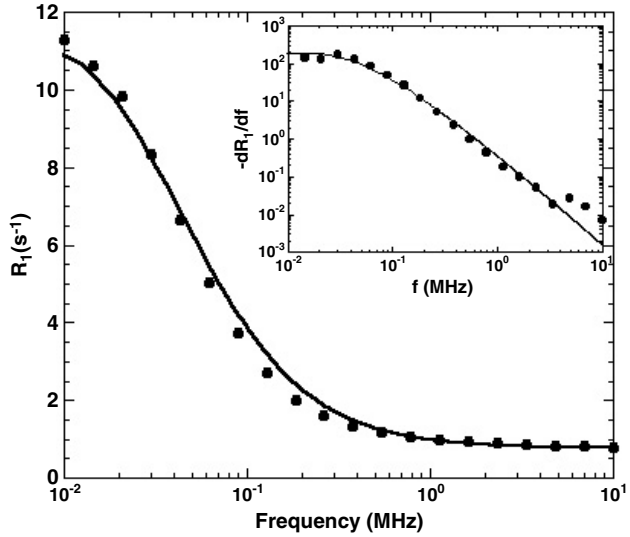

Figure 6. Water spin-lattice relaxation rates in a colloidal glass of laponite versus the Larmor frequency at $T = 298$ K. The particle concentration is 4 w/w. Closed circles: 1H NMR dispersion. Continuous line: theoretical model. The frequency derivative of R_1 is shown in the inset.

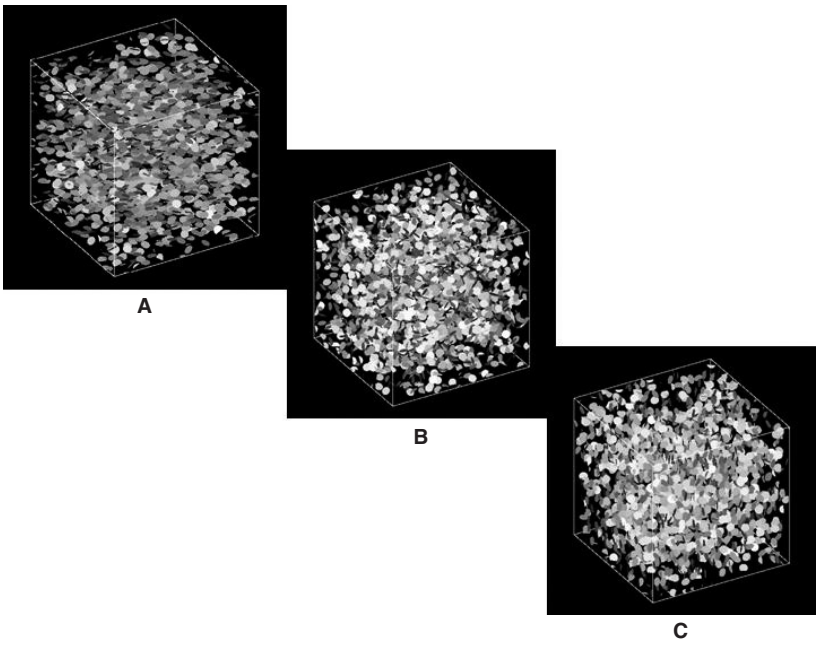

Figure 7. 3D off-lattice reconstruction of laponite suspensions using a simulated annealing algorithm in reciprocal q-space [21, 22]. The particle concentration is 0.028 w/w. A: $S_{ord} = 0.8$. B: $S_{ord} = 0$; C: $S_{ord} = -0.43$.

self-diffusion of the fluid. Each time that a molecule hits the interface, it gets adsorbed for a time τ_A. The self-diffusion coefficient of a water molecule near a disc-like colloid is taken as 5×10^{-10} m^2 s^{-1}.

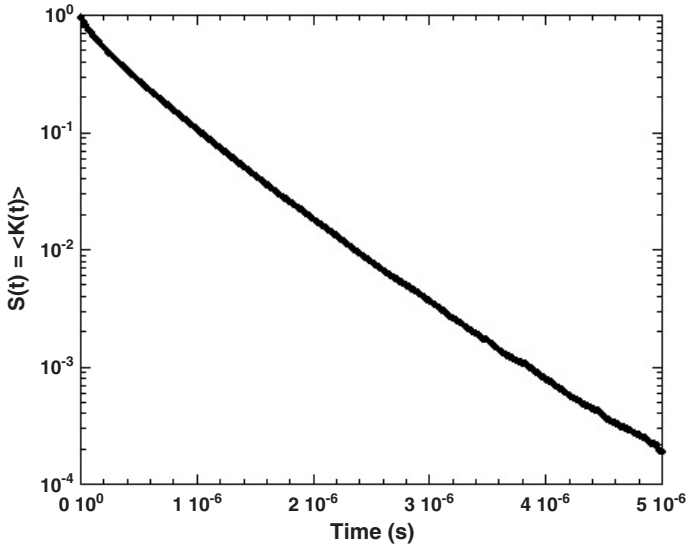

Figure 8. Numerical simulation of the overall survival probability $\langle K(t)\rangle$ inside a 3D off-lattice reconstruction of laponite glasses. The particle concentration is 0.04 w/w. The adsorption time is $\tau_A = 4$ ns. The self-diffusion coefficient of a water molecule near a disc-like colloid is taken as 5×10^{-10} m^2 s^{-1}.

We consider that, at long times and low frequencies, the mean relaxation process is mainly due to intramolecular dipolar interaction as shown in the experiment [10]. This magnetic interaction is computed when the molecule is adsorbed. Otherwise, it is set at zero. In the slow dynamics domain, we compute the spin-lattice relaxation rate according to $R_1^{\text{slow}}(\omega) \propto J_1(\omega) + 4J_2(2\omega)$ with

$$J_{1,2} = (24\pi/5)FT(\langle Y_2^{1,2^*}(\Omega_{LD}(t=0)) \cdot f(t=0) Y_2^{1,2}(\Omega_{LD}(t)) \cdot f(t)\rangle) \tag{19}$$

with $f(t) = 1$ if the molecule is adsorbed on the solid surface and $f(t) = 0$ if not (bulk loop). $\Omega_{LD}(t)$ are the Euler angles between the constant magnetic field $\vec{B}_0$ and the surface director probed by the molecule at time t. The product, inside the brackets, is equal to 0 when the molecule is not adsorbed.

In the glassy state, the low-frequency magnetic relaxation can be induced by three possible processes: (i) the overall survival probability on a defined particle; (ii) the 'orientational memory' between different particles; (iii) the dynamics near the flat and finite interface as discussed in section 3. As shown in figure 8, it is found that the overall survival probability on a defined particle, $\langle K(t)\rangle$, is essentially exponential with an average escaping time, τ_{esc}, around 1 μs. This process cannot justify by itself the experimental evolution shown in figure 6 but only the crossover at small frequencies. In the glassy state and for particle concentration W_t ranging from 0.01 to 0.05, it was numerically found that $(R_1(\omega)/W_t)$ dispersions follow a unique master curve as experimentally observed [10]. Finally, the evolution of $R_1(\omega)$ is not affected by the nematic order of the colloidal suspension (see figure 9) and depends essentially on the confined dynamics of a molecule nearby the surface of a single particle. As shown in figure 9, modulation of the adsorption time τ_A permits us to change drastically the algebraic regime of relaxation. For short adsorption times ($\tau_A = 0.5$ ns), the characteristic exponent of the algebraic regime is close to 0.5 and it moves to higher values (around unity in figure 9)

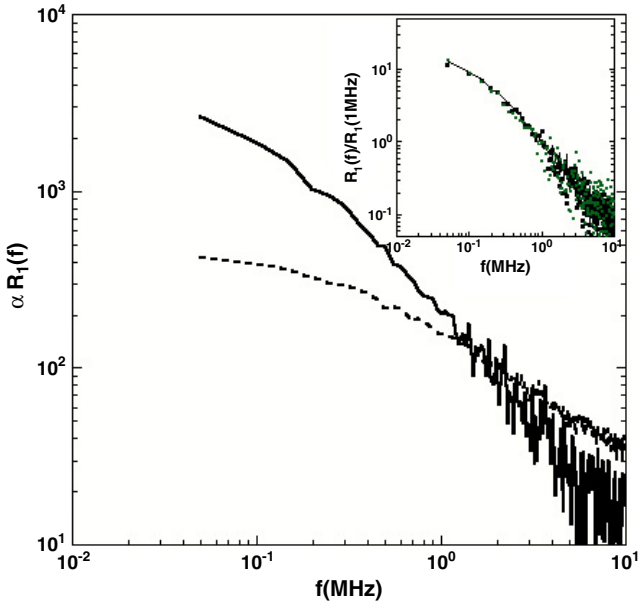

Figure 9. Numerical simulations of NMRD inside a 3D off-lattice reconstruction of laponite glasses at 0.028 w/w. The self-diffusion coefficient of a water molecule near a disc-like colloid is taken as 5×10^{-10} m^2 s^{-1}. Full line: $S_{\mathrm{ord}} = 0$ and $\tau_{\mathrm{A}} = 4$ ns. Dot line: $S_{\mathrm{ord}} = 0$ and $\tau_{\mathrm{A}} = 0.5$ ns. The weak effect of the nematic order is show in the inset for $\tau_{\mathrm{A}} = 4$ ns. Full line: $S_{\mathrm{ord}} = 0$; close points: $S_{\mathrm{ord}} = 0.8$; open points: $S_{\mathrm{ord}} = -0.43$.

(This figure is in colour only in the electronic version)

as τ_{A} increases to 4 ns. These numerical results are in good agreement with our theoretical predictions (see equation (15) and following comments). Indirectly, the exponent variation can provide information about the interaction strength between a molecule and a surface.

These numerical simulations support the theoretical approach developed in section 3.3. This model depends essentially on two independent components. (i) An overall survival probability $\langle K(t) \rangle$ on a defined finite interface. This function takes into account the final orientation memory loss appearing when a molecule leaves definitively a defined particle but not the time fluctuations generated by a random alternation of adsorption steps and bulk loops. Previous numerical simulations show that $\langle K(t) \rangle$ is essentially exponential and can be written as $\langle K(t) \rangle = \exp(-t/\tau_{\mathrm{esc}})$ where τ_{esc} is the average escaping time from a defined flat particle. τ_{esc} imposes the low-frequency crossover. (ii) A crossover frequency ω_0 that imposes the NMRD algebraic regime and its characteristic exponent which is experimentally close to unity. The prediction of this theoretical model is shown (continuous lines) in figure 6 with the two following values: $\tau_{\mathrm{esc}} = 3.5$ μs and $\omega_0 = 0.1$ MHz. We observe a good agreement with experimental data over more than two orders of magnitude in the frequency range. The specific value of ω_0 can be justified if we choose a minimal loop duration of $\tau_{\mathrm{L}} = 10$ ps, something larger that the hydrogen bond lifetime. In this case, the average adsorption time is $\tau_{\mathrm{A}} = 5$ ns. Using the Eyring relationship, this adsorption time is related to a surface activation free energy of about 10 kT, of the same order of magnitude as the experimental heat of immersion [23]. It is possible to give a rough estimation of τ_{esc}, assuming that the main escaping process is the occurrence of Brownian loops having an end to end extension larger than the particle size ξ. We get $\tau_{\mathrm{esc}} = (\xi^2/(6D_w)) + \tau_{\mathrm{A}}\sqrt{\xi^2/(6D_w\tau_{\mathrm{L}})}$. For a diffusion coefficient $D_w = 10^{-9}$ m^2 s^{-1}

and a particle size $\xi = 30$ nm, we find a value of 0.8 μs, which is about the same order of magnitude as predicted by the theoretical model.

5. Surface shape and dimensional crossover

The former results seem to confirm that the probability of the first return to a surface is algebraic and exhibits long-time memory. This noticeable property extends the fluid dynamics near an interface towards the low-frequency domain and has some interesting consequences concerning the long-term surface reactivity of a fluid molecule. We also believe that such characteristics can be used to probe interfacial dynamics by itself, for example in the case of a colloidal system undergoing a phase transition (dynamical arrest, rotational blockage) [10]. The case of a flat surface is really specific and, in most cases, curved, anisotropic or irregular interfaces are encountered. In this last part, we discuss briefly how surface irregularities can affect the loop statistics and induce specific transport properties.

5.1. Surface roughness

In this section, we want to summarize some recent results [25] performed in collaboration with Grebenkov *et al* [25] and concerning the first passage statistics for a random walker starting from a disordered interface and returning to it. Fractal boundaries are considered here as appropriate models to mimic the geometrical irregularity in realistic systems. We wish to investigate how the power-law evolution of $\psi_{\mathrm{L}}(t)$ and $\theta_{\mathrm{L}}(r)$ changes in the case of fractal interfaces. Numerical simulations were carried out in 3D embedding spaces. As a generic self-similar fractal in R^3, we have studied 3D intersections of 4D Weierstrass–Mandelbrot self-affine hypersurfaces [13]. Weierstrass–Mandelbrot functions are also used in three dimensions to generate self-affine interfaces. Starting from a random point located in the interfacial region, an off-lattice diffusive Brownian dynamics simulation is performed to compute the first passage statistics. It is found that basic properties of the first passage statistics strongly evolve with the surface fractal dimension d. In the case of self-similar interfaces, we find that $\psi(t) \sim t^{-\alpha}$ and $\theta(r) \sim r^{-\beta}$ for large enough t and r. For self-affine interfaces, a similar trend is first observed. However, a crossover to a regular flat interface situation ($\alpha = 3/2$ and $\beta = 2$) appears at large r and long times t as shown in figure 10. We have recently found [25] that $\alpha = (d+1)/2$ and $\beta = d$ in three dimensions.

These relationships can be understood if we consider the integrated probability $P_D(t)$ that a random walk launched at $t = 0$ in the bulk hits the boundary interface for the first time at time t. This probability evolves at long times as [4, 24]:

$$P_D(t) \sim t^{-(d+2-d_{\mathrm{e}})/2} \tag{20}$$

where d_{e} is the Euclidean dimension of the embedding space. But $P_D(t)$ can also be considered as the probability for a random walk to escape from the absorbing surface (survive at least until time t). In such conditions, we have

$$\psi_{\mathrm{L}}(t) = -\frac{\mathrm{d}P_D(t)}{\mathrm{d}t}. \tag{21}$$

Then $\alpha = (d+2)/2$ for $d_{\mathrm{e}} = 2$ in agreement with our results.

How robust is the equality $\alpha = (d+1)/2$? The scaling argument (see equation (20)) developed by Maritan [24] is quite general, whatever the geometrical complexity of the surface. It involves the transport at the fractal surface of a volume with linear size L. This observation opens the possibility for the Brownian flights to be sensitive to surface geometrical crossover at long times. This is the case for a self-affine surface (see figure 10). However, such a situation

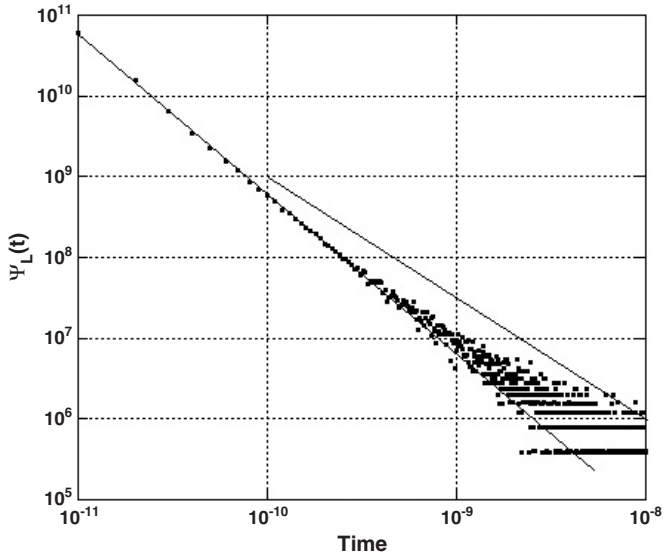

Figure 10. Evolution of the probability density $\psi_L(t)$ that a particle starts from the interface at $t = 0$ and returns to it, for the first time, at time between t and $t + dt$. Case of a self-affine interface in 3D embedding space with $d = 2.85$. The two continuous lines have (in the log–log scale) a slope of -1.95 and -1.5 respectively. A time crossover is observable around 10^{-9}.

could be observed in the case of mass fractal systems with $1 < d < 2$ embedded in 3D Euclidean space: a regular behaviour should be expected at small distances and short times ($\alpha = 3/2$ and $\beta = 2$), followed at larger distances and times by a crossover to $\alpha = (d + 1)/2$ and $\beta = d$. A numerical work is actually underway to check this point. A basic situation exhibiting such an evolution is the case of a long and very thin cylinder ($d = 1$). In the following section, we analyse this specific system.

5.2. Probing colloidal shape

Is it possible to probe a colloidal shape, looking at the slow and confined fluid dynamics near the colloidal surface? Such a question is closely related to Kac's problem [26]: Can one hear the shape of a drum? In the following, we analyse the case of a thin cylindrical colloid (a few nm in diameter). In the local framework of the cylinder shown in figure 11, where $\vec{n}_d$ defines the z axis, the slowest contribution of the magnetic quadrupolar noise $I(t)$ felt by a molecule diffusing near the surface is related to the value of $Y_2^0(\pi/2)$. $I(t)$ exhibits a time evolution apparently similar to the case of a flat surface shown in figure 4. However, Brownian dynamics numerical simulations performed around a unique cylinder do not exhibit an algebraic evolution but a logarithmic one, as shown in figure 12.

This result can be rationalized if we observe that, at short times, a fluid molecule diffusing near the cylinder probes a flat and slightly curved surface. At longer times and larger distances, the colloidal particle appears as a portion of a line. The embedded fluid dynamics is sensitive to this geometrical crossover. Following the former discussion on the equality $\alpha = (d + 1)/2$, $\psi(t) \sim 1/t^{3/2}$ at short times and crosses over to $1/t$ at longer times. This time evolution generates, for $J(\omega)$, a $-\ln(\omega)$ dependence at small frequencies. Such a process should be considered in order to rationalize recent results on magnetic relaxation dispersion of lithium or tetramethyl ammonium in diluted suspensions of DNA [27], where unexpected $-\ln(\omega)$

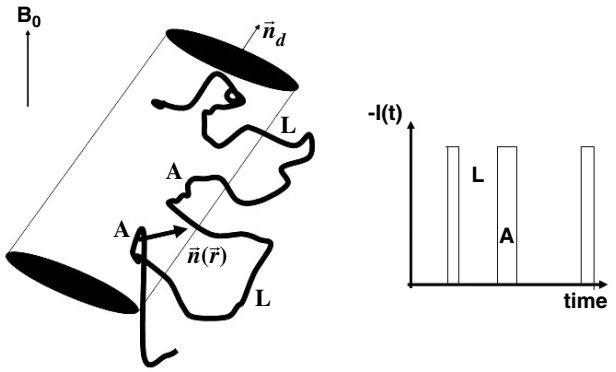

Figure 11. Slow contributions of a magnetic fluctuation $I(t)$ near a cylindrical interface for an intra-dipolar or a quadrupolar interaction. A and L stand for the adsorption stage and the Brownian loop in the bulk, respectively. $\vec{n}(\vec{r})$ stands for the normal vector to the cylindrical surface at position. On the right, the time evolution of the slowest contribution of $I(t)$ in a local framework of the cylinder where $\vec{n}_d$ defines the z-axis.

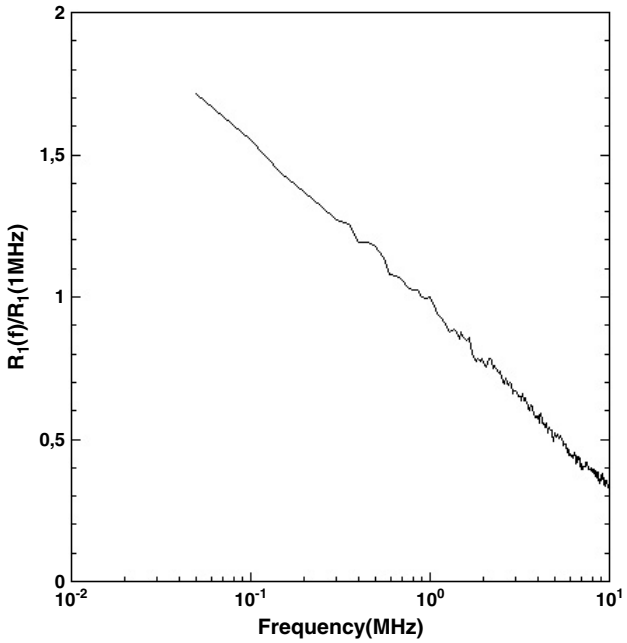

Figure 12. Computation of the spin-lattice relaxation dispersion using a Brownian dynamics simulation around a isolated cylinder having a diameter of 2.5 nm. Slow contributions of a magnetic fluctuation $I(t)$ (intra-dipolar or a quadrupolar interaction) near the cylindrical interface are taken into account. The self-diffusion coefficient of the fluid molecule near the colloid is taken as 5×10^{-10} m^2 s^{-1}. The average adsorption time is $\tau_A = 0.5$ ns.

dependence is observed. Experiments on suspensions of long colloidal thin rods (either mineral or biological) are currently underway in our group in order to check if the slow fluid dynamics near a colloidal interface may provide information about the particle shape.

6. Conclusion

In this paper, we review some statistical properties of random flights in various interfacial confining systems. The statistics of times and displacements between two consecutive interface hits are needed as prerequisites in order to understand the full transport process. This question is related to a first passage problem and plays a central role in various transport phenomena. We analyse some properties of the Brownian flight statistics and discuss how they are involved in self-diffusion processes. We show how surface shape and interface irregularities can affect the loop statistics and induce specific properties at long times. From the experimental point of view, we investigate the slow fluid dynamics near colloidal interfaces by field-cycling NMR relaxometry. It is a way to follow slow dynamical correlations from 1 ns to 10 μs. This spectroscopy appears to be a good choice, considering that the algebraic nature of the probability of the first return to a surface builds a long-time memory. The experimental part confirms that the embedded fluid dynamics is sensitive to possible morphologic crossover and provide information about interface geometry. We also believe that such an approach can be used to probe interfacial dynamics by itself, for example in the case of a colloidal system undergoing a phase transition (dynamical arrest, rotational blockage, . . .).

Further works are underway in our group to check these points and to clarify several problems related to surface accessibility, dynamical bias induced by a long-range surface field and finally possible correlation between successive Brownian flights in an intricate interfacial geometry.

Acknowledgments

The author wishes to acknowledge collaboration and valuable discussions with D Grebenkov, K Kolvankar, B Sapoval and J-P Korb.

References

[1] Shlesinger M F, Klafter J and Zumofen G 1999 *Am. J. Phys.* **67** 1253
[2] Sapoval B 1994 *Phys. Rev. Lett.* **73** 3314
[3] Redner S 2001 *A Guide to First Passage Processes* (Cambridge: University Press)
[4] Duplantier B 1991 *Phys. Rev. Lett.* **66** 1555
Duplantier B 2000 *Phys. Rev. Lett.* **84** 1363
[5] Golstein R E, Hasley T C and Leibig M 1991 *Phys. Rev. Lett.* **66** 1551
[6] Blanco S and Fournier R 2003 *Europhys. Lett.* **61** 168
[7] Mazollo A 2004 *Europhys. Lett.* **68** 350
[8] Benichou O, Coppey M, Moreau M, Suet P H and Voituriez R 2005 *Europhys. Lett.* **70** 42
[9] Stapf S, Kimmich R and Seitter R O 1995 *Phys. Rev. Lett.* **75** 2855
[10] Levitz P and Korb J-P 2005 *Europhys. Lett.* **70** 672
[11] Levitz P and Tchoubar D 1992 *J. Physique* I **2** 771
[12] Levitz P 1993 *J. Phys. Chem.* **97** 3813
[13] Levitz P 1997 *Europhys. Lett.* **39** 593
[14] Feller W 1968 *An Introduction to Probability Theory and its Applications* (New York: Wiley)
[15] Bychuk O V and O'Shaughnessy B 1995 *Phys. Rev. Lett.* **74** 1795
[16] Bychuk O V and Shaughnessy B O 1994 *J. Physique* II **4** 1135
[17] Korb J-P, Whaley-Hodges M and Bryant R G 1997 *Phys. Rev.* E **56** 1934
[18] Halle B and Wennerstrom H 1981 *J. Chem. Phys.* **75** 1928
[19] Levitz P, Lécolier E, Mourchid A, Delville A and Lyonnard S 2000 *Europhys. Lett.* **49** 672
[20] Zavada T, Kimmich R, Grandjean J and Kobelov A J 1999 *J. Chem. Phys.* **110** 6977
[21] Rintoul M and Torquado S J 1997 *Colloid Interface Sci.* **186** 467

[22] Levitz P 2002 *Handbook of Porous Media* ed K Sing (New York: Wiley–VCH) chapter 2 (Statistical Modeling of Pore Network)
[23] Fripiat J, Cases J M, Francois M and Lettelier M 1982 *J. Colloid Interface Sci.* **89** 378
[24] Maritan A, Stella A L and Toigo F 1989 *Phys. Rev.* B **40** 9269
[25] Levitz P, Grebenkov D S, Kolvankar K and Sapoval B 2005 *Phys. Rev. Lett.* submitted
[26] Kac M 1966 *Am. Math. Month.* **73S** 1
[27] Victor K G, Teng C L, Diensen T R D, Korb J-P and Bryant R G 2004 *Magn. Reson. Chem.* **42** 518